THE JOURNAL OF BIOLOGICAL CHEMISTRY VOL. 289, NO. 18, pp. 12693–12704, May 2, 2014
© 2014 by The American Society for Biochemistry and Molecular Biology, Inc. Published in the U.S.A.

Ribosomes in a Stacked Array

*ELUCIDATION OF THE STEP IN TRANSLATION ELONGATION AT WHICH THEY ARE STALLED DURING S-ADENOSYL-L-METHIONINE-INDUCED TRANSLATION ARREST OF CGS1 mRNA**

Received for publication, October 14, 2013, and in revised form, March 7, 2014 Published, JBC Papers in Press, March 20, 2014, DOI 10.1074/jbc.M113.526616

Yui Yamashita[‡], Yoshitomo Kadokura[‡1], Naoyuki Sotta[§], Toru Fujiwara[§], Ichigaku Takigawa[¶], Akiko Satake[‖], Hitoshi Onouchi[**], and Satoshi Naito[‡2]**

*From the [‡]Division of Life Science, Graduate School of Life Science, Hokkaido University, Sapporo 060-8589, Japan, the [§]Department of Applied Biological Chemistry, Graduate School of Agricultural and Life Sciences, The University of Tokyo, Tokyo 113-8657, Japan, the [¶]Creative Research Institution, Hokkaido University, Sapporo 001-0021, Japan, the [‖]Biosphere Department, Graduate School of Environmental Science, Hokkaido University, Sapporo 060-0810, Japan, and the **Division of Applied Bioscience, Graduate School of Agriculture, Hokkaido University, Sapporo 060-8589, Japan*

Background: *S*-Adenosyl-L-methionine arrests ribosomes on *CGS1* mRNA at the pre-translocation step, and ribosomes stack behind it.
Results: Puromycin reactivity of stacked ribosomes was intermediate between ribosomes at the pre- and post-translocation steps.
Conclusion: Ribosomes are stacked at nine-codon intervals, and the majority are stalled at an early step of translocation.
Significance: This study is the first report of ribosomal states in a stacked array.

Expression of *CGS1*, which codes for an enzyme of methionine biosynthesis, is feedback-regulated by mRNA degradation in response to *S*-adenosyl-L-methionine (AdoMet). *In vitro* studies revealed that AdoMet induces translation arrest at Ser-94, upon which several ribosomes stack behind the arrested one, and mRNA degradation occurs at multiple sites that presumably correspond to individual ribosomes in a stacked array. Despite the significant contribution of stacked ribosomes to inducing mRNA degradation, little is known about the ribosomes in the stacked array. Here, we assigned the peptidyl-tRNA species of the stacked second and third ribosomes to their respective codons and showed that they are arranged at nine-codon intervals behind the Ser-94 codon, indicating tight stacking. Puromycin reacts with peptidyl-tRNA in the P-site, releasing the nascent peptide as peptidyl-puromycin. This reaction is used to monitor the activity of the peptidyltransferase center (PTC) in arrested ribosomes. Puromycin reaction of peptidyl-tRNA on the AdoMet-arrested ribosome, which is stalled at the pre-translocation step, was slow. This limited reactivity can be attributed to the peptidyl-tRNA occupying the A-site at this step rather than to suppression of PTC activity. In contrast, puromycin reactions of peptidyl-tRNA with the stacked second and third ribosomes were slow but were not as slow as pre-translocation step ribosomes. We propose that the anticodon end of peptidyl-tRNA resides in the A-site of the stacked ribosomes and that the stacked ribosomes are stalled at an early step of translocation, possibly at the P/E hybrid state.

An actively translating mRNA bears many ribosomes as a polysome complex. When one ribosome stalls, the following ones will form a stacked array behind it. Polysomes have been extensively studied because of their contribution to overall translation activity (1–7). In contrast, reports on stacked ribosomes are limited (8). However, they are not static but sometimes play a role in the control of gene expression. One such example occurs in the *Arabidopsis CGS1* gene, which encodes the first committed enzyme in methionine biosynthesis. Expression of *CGS1* is negatively feedback-regulated by its mRNA degradation in response to *S*-adenosyl-L-methionine (AdoMet),[3] a direct metabolite of methionine (9, 10). The amino acid sequence of the MTO1 region in *CGS1* acts as the *cis* element in this response. Studies using an *in vitro* translation system of wheat germ extract (WGE) revealed that, in the presence of AdoMet, the nascent MTO1 peptide induces translation arrest at the Ser-94 codon located immediately downstream of the MTO1 region, causing peptidyl-tRNA^{Ser} (PtR^{Ser}) to accumulate (11). Subsequently, several ribosomes stack behind the AdoMet-arrested one, and multiple mRNA degradation events occur to produce a ladder of 5′-truncated RNA species as degradation intermediates, most likely through the action of an endoribonuclease, suggesting that the stacked ribosomes function in determining the sites of *CGS1* mRNA degradation (12).

In the AdoMet-arrested ribosome, PtR^{Ser} resides in the A-site of the small subunit (11), implying that the ribosome

* This work was supported by a Grant-in-Aid for Japan Society for the Promotion of Science Fellows 23-1971 (to Y. Y.) from the Japan Society for the Promotion of Science; by a Grant-in-Aid for Scientific Research on Innovative Areas 22119006 (to S. N.) from the Ministry of Education, Culture, Sports, Science, and Technology of Japan, and Core Research for Evolutionary Science and Technology (CREST) Grant PJ34085001 (to H. O.) from the Japan Science and Technology Agency.
[1] Present address: Research Institute for Bioscience Products and Fine Chemicals, Ajinomoto Co., Inc., Kawasaki 210-8681, Japan.
[2] To whom correspondence should be addressed: Division of Applied Bioscience, Graduate School of Agriculture, Hokkaido University, Sapporo 060-8589, Japan. Tel.: 81-11-706-2800; Fax: 81-11-706-4932; E-mail: naito@abs.agr.hokudai.ac.jp.

[3] The abbreviations used are: AdoMet, *S*-adenosyl-L-methionine; CHX, cycloheximide; nt, nucleotide(s); PTC, peptidyltransferase center; PtR, peptidyl-tRNA; WGE, wheat germ extract.

TABLE 1

Plasmids used for *in vitro* transcription and PCR primers used for their construction

Mutagenesis methods used are: o, overlap extension PCR method; i, inverse PCR.

Plasmid	Mutation	Forward primer (5′-3′)	Reverse primer (5′-3′)	Mutagenesis
***M8:Ex1*(*WT*)-based synonymous codon substitutions**				
pYY23	Ile-74(AUA)	TGAGCATAAAAGCCCGTAGAA	GGCTTTTATGCTCAGCTGAC	o
pYY22	Lys-75(AAG)	GCATTAAGGCCCGTAGAAACT	ACGGGCCTTAATGCTCAGCT	o
pYY24	Ala-76(GCG)	TAAAGCGCGTAGAAACTGTAGC	TCTACGCGCTTTAATGCTCAG	o
pYY25	Ala-76(GCA)	TAAAGCACGTAGAAACTGTAGC	TCTACGTGCTTTAATGCTCAG	o
pYY26	Arg-77(CGG)	TAAAGCCCGGAGAAACTGTAGC	GTTTCTCCGGGCTTTAATGC	o
pYY28	Arg-77(AGG)	TAAAGCCAGGAGAAACTGTAGC	GTTTCTCCUGGCTTTAATGCTCAG	o
pYY27	Arg-77(AGA)	TAAAGCCAGAAGAAACTGTAGC	GTTTCTUCUGGCTTTAATGCTCAG	o
pYY21	Ile-83(AUA)	ACATAGGTGTTGCACAGATCG	GCAACACCTATGTTGCTACAG	o
pYY20	Gly-84(GGG)	ATCGGGGTTGCACAGATCG	GCAACCCCGATGTTGCTAC	o
pYY19	Gly-84(GGA)	ATCGGAGTTGCACAGATCG	GCAACTCCGATGTTGCTAC	o
pYY17	Val-85(GUG)	CGGTGTGGCACAGATCG	TGTGCCACACCGATGTTGC	o
pYY18	Val-85(GUA)	CGGTGTAGCACAGATCG	TGTGCCACACCGATGTTGC	o
pYY43	Ser-94(UCG)	CTAAGTGGTCGAACAACCCATC	GGTTGTTCGACCACTTAGC	o
pYY44	Ser-94(AGC)	CTAAGTGGAGCAACAACCCATC	GGTTGTTGCTCCACTTAGC	o
***M8:ND5*(*C80A*)-based cysteine substitutions**				
pYY37	K75C, C80A	TTTAATGCTCAGCTGACGGAC	TGTCGTAGAAACGCTAGCAACATC	i
pYY38	A76C, C80A	TGTGCCCGTAGAAACGCTAGCAA	AATGCTCAGCTGACGGACGA	i
pYY39	R77C, C80A	TGAGCATTAAAGCCTGTAGAAAC	CAGTTTCTACAGGCTTTAATGCTC	o
pYY40	R78C, C80A	AAGCCCGTTGTAACGCTAG	TGCTAGCGTTACAACGGGCT	o
pYY41	N79C, C80A	AAGCCCGTAGATGTGCTAGCAA	TTGCTAGCACATCTACGGGCTT	o
pYY42	K92C, C80A	GCGGCTTGTTGGTCCAACAAC	GGACCAACAAGCCGCCACGAT	o

stalls during the translocation step. AdoMet-induced arrest of *CGS1* mRNA translation is temporary, and resumption of this translation can be blocked by cycloheximide (CHX), which inhibits ribosomal translocation (11). A recent report revealed that CHX blocks movement of the deacylated tRNA toward the E-site within the large subunit at an early step of translocation (13). This enables reinterpretation of our previous data as demonstrating that AdoMet induces translation arrest at the pre-translocation step in *CGS1*.

Stacking of ribosomes also occurs during normal translation termination (8); however, no report has linked this stacking to mRNA degradation. A ladder of possible mRNA degradation intermediates similar to those of *CGS1* was recently reported in the no-go mRNA decay system in yeast (14), possibly also suggesting a role of stacked ribosomes in mRNA degradation. Under what conditions do the stacked ribosomes take part in mRNA degradation? To answer this question, we must better understand the stacked array of ribosomes. RNase protection experiments have indicated that mRNA protected by a stacked ribosome is 27–29 nucleotides (nt) in length (8), suggesting that ribosomes are arranged at either nine- or ten-codon intervals in a stacked array. However, the step in the translation elongation cycle at which the stacked ribosomes are stalled has not been studied. Also, the exact intervals of the ribosomes in a stacked array have not been reported in terms of codons.

In the present study, we addressed two questions: (i) where are the stacked ribosomes located relative to the arrested ribosome, and (ii) at which step in the translation elongation cycle are the stacked ribosomes stalled? Primer extension inhibition (toeprint) experiments are used to determine the location of an arrested ribosome on a mRNA, based on the established distance between the P-site of the small subunit and toeprint signal (15, 16), but the location of the stacked ribosomes must be identified by other methods. Here, we determined the tRNA species of the PtRs in the stacked ribosomes and analyzed the puromycin reactivity of AdoMet-arrested and stacked ribosomes. Puromycin, an analog of aminoacyl-tRNA, binds to the A-site of the peptidyltransferase center (PTC) and reacts with PtR in the P-site, releasing the nascent peptide as peptidyl-puromycin. To deduce the ribosomal location on the mRNA by identifying PtR species, occupation of PtR in the A- or P-site of the small subunit must be determined. Because puromycin reactivity of PtR changes depending on the step in the translation elongation cycle, integrating the results of PtR location on mRNA and the arrested step is required. Therefore, our two questions are mutually interrelated.

EXPERIMENTAL PROCEDURES

Chemicals—AdoMet was purchased from Sigma-Aldrich (iodide salt, A4377; St Louis, MO, USA) and puromycin from Wako Pure Chemicals (Osaka, Japan). Edeine was a gift from the National Cancer Institute (Bethesda, MD, USA). Sources of other chemicals were previously reported (17).

Plasmids—pYK00 and pYK01 carry *M8:Ex1*(*WT*) and *M8:Ex1*(*mto1–1*) DNA, respectively, in the pSP64 poly(A) vector (Promega, Madison, WI, USA) (17). pNO57 carries *M8:ND5*(*C80A*) DNA in pSP64 poly(A) (17).

Plasmids pYY17 through pYY28, pYY43, and pYY44 carry synonymous codon substitutions of *M8:Ex1*(*WT*) (Table 1). *In vitro* mutagenesis was accomplished by the overlap extension PCR method (18, 19). The XbaI-BamHI fragment containing the wild-type *CGS1* exon 1 coding region of pYK00 was replaced with the XbaI-BamHI fragment generated by overlap extension PCR of pYK00 DNA using PrimeSTAR HS DNA polymerase (Takara Bio, Ohtsu, Japan). The franking primers used for overlap extension PCR were described (17). Plasmids pYY37 through pYY42 carry cysteine substitutions of *M8:ND5*(*C80A*) (Table 1). Except for pYY37 and pYY38, *in vitro* mutagenesis was accomplished by the overlap extension PCR method as above using pNO57 as a template. *In vitro* mutagenesis for pYY37 and pYY38 plasmids was accomplished by inverse PCR using KOD Plus Neo DNA polymerase

(Toyobo, Tokyo, Japan) followed by digestion of the plasmid DNA by DpnI (Toyobo) using pNO57 as a template. Then, PCR products were self-ligated using T4 DNA ligase (Wako Pure Chemicals) and T4 polynucleotide kinase (Toyobo). Primers used for *in vitro* mutagenesis are shown in Table 1. In all cases, the mutations were confirmed by DNA sequencing.

In Vitro Transcription—In vitro transcription of *M8:Ex1*(*WT*), *M8:ND5*(*C80A*), and their derivatives by SP6 RNA polymerase (CellScript, Madison, WI) in the presence of a cap analog was carried out as described previously (17). DNA templates for *nonstop* RNAs, *M8:Ex1*(*S94ns*) and *M8:Ex1*(*V85ns*), were prepared by PCR amplification of corresponding regions from pYK00 using PrimeSTAR HS DNA polymerase. The forward primer used was SP65′fP (17). The reverse primers used for *M8:Ex1*(*S94ns*) and *M8:Ex1*(*V85ns*) were S94r (17) and 5′-AACACCGATGTTGCTACAGT-3′ (V85r), respectively. DNA template for *M8:Ex1*(*mto1–1*, *S94ns*) was prepared as for *M8:Ex1*(*S94ns*), except that pYK01 was used instead of pYK00. The amplified fragments were used for *in vitro* transcription as described previously (17).

In Vitro Translation—In vitro translation reactions using WGE (Promega) were carried out as described (10), except for adding [^{35}S]methionine or [^{35}S]cysteine (37 TBq mmol^{-1}, 370 MBq ml^{-1}, American Radiolabeled Chemicals, St. Louis, MO) in the translation reaction mixture. *M8:Ex1* RNA (1 pmol) or *nonstop* RNA (2 pmol) was translated in a 20-μl WGE reaction mixture in the presence or absence of 1 mM AdoMet. The reaction mixture for the [^{35}S]methionine labeling experiment consisted of 10 μl of WGE, 1.6 μl of a 1 mM amino acid mixture lacking methionine (Promega), 0.3 μl 5 μM L-methionine, and 0.06 μl of [^{35}S]methionine. For [^{35}S]cysteine labeling, the reaction mixture consisted of 10 μl of WGE, 1.6 μl of a 1-mM amino acid mixture lacking methionine and cysteine (Promega), 0.4 μl of 5 μM L-methionine, and 0.5 μl of [^{35}S]cysteine. RNase A treatment was performed as described (11). Translation samples were boiled for 3 min, separated on a NuPAGE 4–12% BisTris gel in MOPS running buffer (Invitrogen, Carlsbad, CA), dried, and visualized using a FLA-7000 image analyzer (Fuji Photo Film, Tokyo, Japan). Because migration of PtRs is affected by temperature, SDS-PAGE was carried out in a 28 °C chamber. Measurements of band intensities and digital data acquisition were carried out using MultiGauge software (Fuji Photo Film).

Puromycin Reaction—For puromycin reaction of PtR, *in vitro* translation was carried out in a 40-μl translation reaction mixture. After 30 min of translation at 25 °C, puromycin was added to a final concentration of 2 mM and further incubated at 25 °C until an aliquot was sampled for SDS-PAGE. The unreacted PtR band was quantified, and the puromycin reactivity was assessed by dividing the band intensity at a given time point by the intensity at time 0.

To test the effect of exogenously added MTO1 peptide on puromycin reactivity, *in vitro* translation and puromycin reaction were carried out in the presence of 500 nM synthetic peptide.

Primer Extension Experiment—Primer extension of RNA after translation in WGE was carried out as described (12).

Pseudo-First-Order Kinetic Analysis of Puromycin Reaction and Statistical Analysis—Puromycin reaction will follow pseudo-first order kinetics provided that puromycin is present in large excess relative to the stalled ribosome (20, 21), as in the present study. In simple first-order kinetics, the amount of unreacted PtR will follow (Equation 1),

$$y = \exp(-k_{app}\, t) \quad \text{(Eq. 1)}$$

where y is amount of the unreacted PtR, k_{app} is the apparent rate constant of puromycin reaction, and t is reaction time.

If PtR consists of two or three PtR species with different k_{app}, the amount of the unreacted PtR will follow a two-component (Equation 2) or three-component (Equation 3) model, and will give a curved line on a semi-log plot.

$$y = f_1\exp(-k_{app\text{-}1}\, t) + (1 - f_1)\exp(-k_{app\text{-}2}\, t) \quad \text{(Eq. 2)}$$

$$y = f_1\exp(-k_{app\text{-}1}\, t) + f_2\exp(-k_{app\text{-}2}\, t) + (1 - f_1 - f_2)\exp(-k_{app\text{-}3}\, t) \quad \text{(Eq. 3)}$$

where f_i is the fraction of i-th component of PtR, and $k_{app\text{-}i}$ is the apparent rate constants of puromycin reaction of i-th component of PtR. Fitting to these models by non-linear least square method was carried out by using Mathematica ver. 9 software (Wolfram Research, Champaign, IL, USA). The Akaike information criterion (22) was used to choose the best fitted model among (Equation 1) - (Equation 3). The rate of spontaneous hydrolysis of PtR was analyzed by (Equation 1).

Statistical analyses were carried out using Welch's *t* test. For multiple comparisons, the false discovery rate correction of Benjamini and Hochberg (23) was applied.

RESULTS

Identification of the Peptidyl-tRNA Band That Was Formed on the AdoMet-arrested Ribosome—In the *in vitro* translation condition used in this study (50 fmol RNA μl^{-1} translation mixture), three major translation arrest products were detectable (Fig. 1), and we previously determined that at least two additional ribosomes were stacked behind the arrested ribosome (12). To identify the stalled sites of the stacked ribosomes, we first identified the PtR of the arrested ribosome. *M8:Ex1*(*WT*) RNA (Fig. 1*A*) was translated in WGE in the presence of [^{35}S]methionine, and the translation products were analyzed by SDS-PAGE. *M8* is a small tag that encodes eight consecutive methionine residues (17, 24). When *M8:Ex1*(*WT*) RNA was translated in the presence of AdoMet, three PtR bands were detected at ~30 kDa, whereas no such band was observed when RNA was translated in the absence of AdoMet (Fig. 1*B*, *lanes 2* and *1*, respectively). We designated these bands PtR(a), PtR(b), and PtR(c) according to their gel mobilities. RNase A treatment of the translation products caused these bands to disappear, and new bands of ~10 kDa were detected that corresponded to the molecular weights of the arrested peptides (Fig. 1*B*, *lane 5*).

When the amount of mRNA increases, fewer ribosomes are expected to load on one mRNA, and fewer ribosomes will stack upon translation arrest. When the concentration of *M8:Ex1*(*WT*) RNA in the translation reaction mixture was increased, the

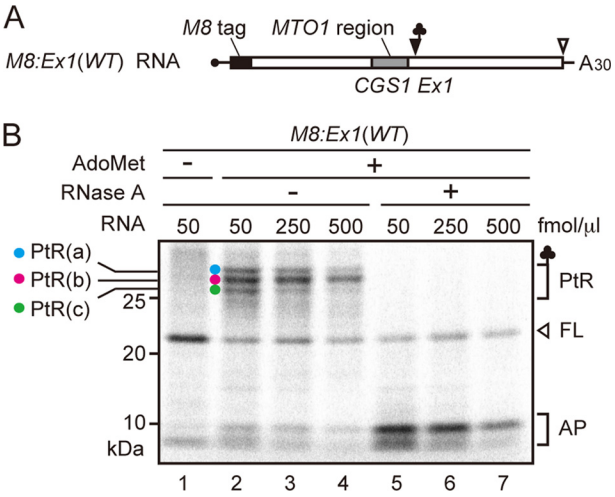

FIGURE 1. **Detection of the three translation arrest products.** *A*, schematic representation of *M8:Ex1*(*WT*) RNA. *B*, detection of three PtRs by SDS-PAGE. *M8:Ex1*(*WT*) RNA (50–250 fmol μl^{-1}, as indicated) was translated in the absence (*lane 1*) or presence (*lanes 2–7*) of 1 mM AdoMet. After 30 min of translation, samples were treated with RNase A (*lanes 5–7*). The AdoMet-dependent PtR (~30-kDa), the 21-kDa full-length translation product (*FL*), and the 10-kDa arrested peptide bands (*AP*) produced by the RNase A treatment are marked. PtR(a), *blue circle*; PtR(b), *magenta circle*; PtR(c), *green circle*. A representative result of triplicated experiments is shown.

intensities of the PtR(a) and PtR(c) bands decreased, whereas that of PtR(b) barely changed (Fig. 1*B*, *lanes 2–4*), suggesting that PtR(b) is PtR^{Ser} formed on the AdoMet-arrested ribosome that stopped at the Ser-94 codon, whereas PtR(a) and PtR(c) were formed on the stacked second or third ribosomes.

To verify these band assignments and to determine the stalled sites of the stacked ribosomes, we performed a gel mobility shift assay. Mobility of PtRs in SDS-PAGE depends on the tRNA species of the PtR, even though the peptide part is the same. Therefore, by changing the codon at the stalled site of the stacked ribosome, we expect a mobility shift of the arrest products, allowing us to determine the PtR species. Because the stalled site of the second stacked ribosome is expected to reside within the MTO1 region, where only limited amino acid changes are allowed (25), we introduced synonymous codon substitutions.

We substituted the wild-type Ser-94(*UCC*) codon with *UCG* or *AGC* codons (Fig. 2*A*). When these RNAs were translated in the presence of AdoMet, the PtR(b) band disappeared (Fig. 2*B*, *lanes 2–4*, *magenta circle*). In the case of Ser-94(*UCG*), a new band, PtR(b1), appeared that was larger than PtR(a) (Fig. 2*B*, *lane 3*, *magenta triangle*), whereas with Ser-94(*AGC*), a new band, PtR(b2), appeared slightly above the PtR(a) band (Fig. 2*B*, *lane 4*, *magenta square*). The results unequivocally determined that PtR(b) was formed on the ribosome that arrested at the Ser-94 codon. Hereafter, we refer to PtR(b) as PtR(S94).

The Stacked Second Ribosome Stalls at Val-85—An RNase protection assay with stacked ribosomes in WGE (8) suggested that ribosomes are stacked at nine- or ten-codon intervals. Therefore, we introduced synonymous codon substitutions at the Ile-83, Gly-84, and Val-85 codons (Fig. 2*A*). Synonymous substitution of Val-85(*GUU*) to *GUG* or *GUA* codons shifted the mobility of PtR(a). When *M8:Ex1*(Val-85 *GUG*) RNA was translated, the resulting PtR(a1) band migrated slightly faster than PtR(a) (Fig. 2*C*, *lane 3*, *blue triangle*). Likewise, when *M8:Ex1*(Val-85 *GUA*) RNA was translated, PtR(a) disappeared, whereas the new PtR(a2) overlapped with PtR(b) (Fig. 2*C*, *lane 4*, *blue square*). Introduction of synonymous codon substitutions at the Ile-83 and Gly-84 codons did not result in PtR mobility shifts (Fig. 2*D*). These results indicate that PtR(a) was formed on the stacked second ribosome and that this ribosome stalled at the Val-85 codon, nine codons upstream of Ser-94. Hereafter, we refer to PtR(a) as PtR(V85).

The Majority of Stacked Third Ribosomes Stalls at Ala-76—We tested synonymous codon substitutions for the Ile-74, Lys-75, Ala-76, and Arg-77 codons to identify where the third ribosome stalled (Fig. 2*A*). The only difference that we detected was a new band, PtR(c1), that migrated faster than PtR(c), when Ala-76(*GCC*) was substituted to *GCA* (Fig. 2*E lane 6*, *green triangle*). Because PtR(c) did not disappear with this substitution, we verified the stalled site of the third ribosome by another approach.

Cysteine substitutions were introduced to *M8:ND5*(*C80A*) RNA, which carries no cysteine residue within *CGS1* exon 1 (Fig. 2*F*) (17), and the translation products were labeled with [^{35}S]cysteine. When *M8:ND5*(*C80A*) RNAs carrying a single cysteine residue at Lys-75 or Ala-76 were translated in the presence of AdoMet, three PtR bands were detected (Fig. 2*G*, *lanes 1* and *2*), indicating that Lys-75 and Ala-76 codons were translated by the third ribosome. In contrast, *M8:ND5* RNAs carrying a single cysteine at Arg-77, Arg-78, Asn-79, and Cys-80 produced two PtR bands (Fig. 2*G*, *lanes 3–6*), showing that these codons were not translated by the third ribosome. These results corroborate the findings of our synonymous codon substitution experiments (Fig. 2*E*) that the third ribosome translates up to Ala-76 codon.

The PtR bands were weak in *M8:ND5*(*R78C*, *C80A*). The Arg-78 to cysteine substitution probably affected AdoMet-dependent translation arrest, because Arg-78 is located within the MTO1 region. A similar case was also observed in *M8:ND5*(*K75C*, *C80A*), in which three PtRs were observed, but the PtR(c) band was weak. Possibly, although Lys-75 was outside the MTO1 region and an alanine substitution was tolerated at this position (25), substitution to cysteine may have affected the translation arrest at Ser-94.

Because PtR(c) did not disappear with the Ala-76(*GCC*) to *GCA* substitution, there may be ambiguity in the stall site of the third ribosome, and/or PtR of the stacked fourth ribosome may overlap with PtR(c); however, these factors would be minor, because the PtR(c) band produced by *M8:ND5*(*A76C*, *C80A*) RNA (Fig. 2*G*, *lane 2*) was as intense as that detected by translation of *M8:Ex1*(*WT*) RNA in the presence of AdoMet (Fig. 2*H*). Alternatively, the Ala-76 codon may be recognized by more than one tRNA species; however, this would not affect the band assignment of PtR(c). Taken together, the results indicated that the majority of stacked third ribosomes translated up to the Ala-76 codon. Hereafter, PtR(c) will be referred to as PtR(A76).

Puromycin Reactivity of the AdoMet-arrested Ribosome—To gain insight into the state(s) of the ribosomes in a stacked array, the puromycin reactivity was analyzed (Fig. 3). The rate of spontaneous hydrolysis of PtR under our experimental conditions was slow enough not to hinder the puromycin reaction assay (Fig. 3, *B* and *F*). *M8:Ex1*(*WT*) RNA was translated in WGE

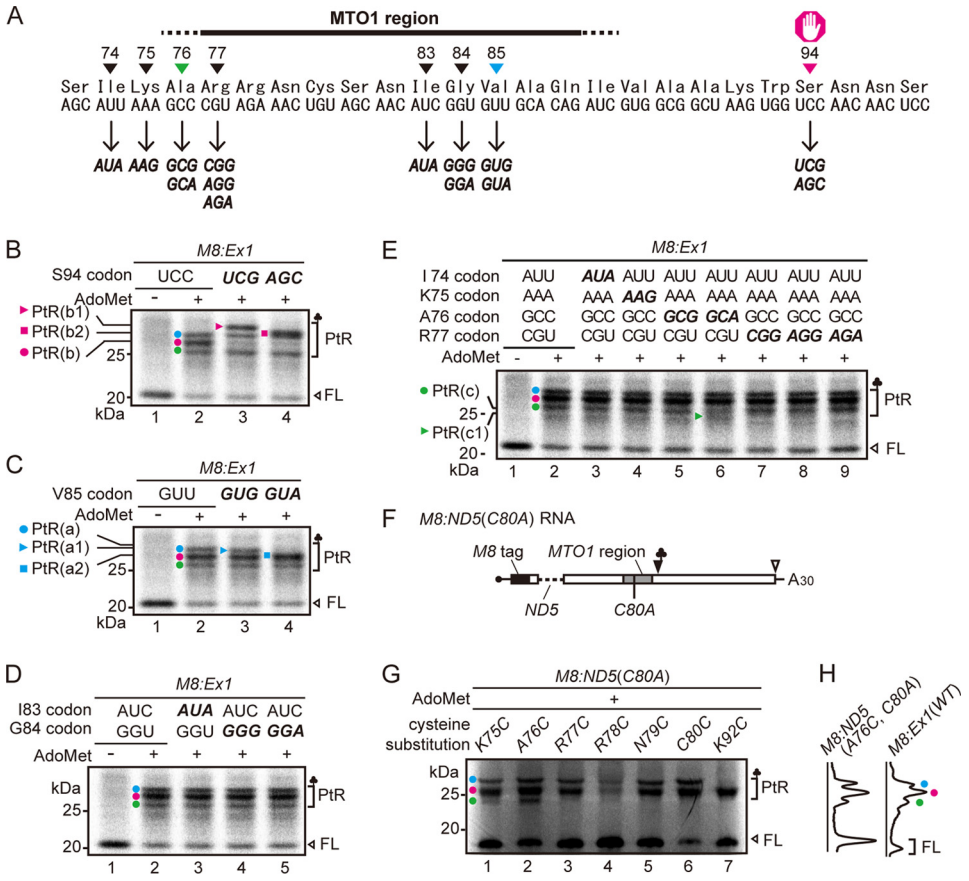

FIGURE 2. **Mapping of the stall sites of arrested and stacked ribosomes.** *A*, nucleotide and amino acid sequences around the MTO1 region. Synonymous codon substitutions were generated at the sites marked. *B–E*, SDS-PAGE analysis of the translation products of *M8:Ex1* RNA (50 fmol μl^{-1}) in the absence (−) or presence (+) of 1 mM AdoMet. The AdoMet-dependent PtR and the full-length translation product (*FL*) are marked. PtR(a), *blue circle*; PtR(b), *magenta circle*; PtR(c), *green circle*. Representative results of triplicated experiments are shown. *B*, effects of synonymous substitutions at the Ser-94 codon. PtR(b1) (*magenta triangle*) and PtR(b2) (*magenta square*) bands are marked. *C* and *D*, The Val-85 codon (*C*) and the Gly-84 and Ile-83 codons (*D*) were synonymously substituted. PtR(a1) (*blue triangle*) and PtR(a2) (*blue square*) bands are marked in *C*. *E*, the codons from Ile-74 to Arg-77 were synonymously substituted. PtR(c1) (*green triangle*) band is marked. *F*, schematic representation of *M8:ND5*(*C80A*) RNA. The region of the *CGS1* exon 1 that was absent in the *ND5* deletion (25) is indicated by a *dashed line*. The Cys-80 to alanine substitution is shown (*C80A*). *G*, cysteine-scanning experiment to detect [^{35}S]cysteine-labeled PtRs. *M8:ND5*(*C80A*) RNAs (50 fmol μl^{-1}) carrying only one cysteine codon at the indicated amino acid positions were translated in the presence of 1 mM AdoMet and subjected to SDS-PAGE analysis. Positions of the AdoMet-dependent PtR and the full-length translation product (*FL*) are marked. *C80C* carries the original cysteine codon. A representative result of duplicated experiments is shown. *H*, scanned images of *E*, *lane 2*, and *G*, *lane 2* are presented.

in the presence of AdoMet for 30 min, and then 2 mM puromycin was added and the time course of puromycin reaction was analyzed. Because excess puromycin was added relative to the stalled ribosome, the reaction will follow pseudo-first order kinetics (20, 21) (Equation 1, "Experimental Procedures"). Simple pseudo-first order kinetics will give a straight line on a semi-log plot, but the line was curved (Fig. 3*F*). This fact can be interpreted, regarding the puromycin reactivity, as indicating that the PtRs are composed of a mixture of fast-reacting and slow-reacting ribosomes (Equation 2, "Experimental Procedures"). Fitting to the two-component model by the least-square method showed that PtR(S94) is composed of ~10% fast-reacting PtR with k_{app} of ~0.6 s^{-1} (hereafter, referred to as $k_{app}[S94^{fast}]$) and 90% slow-reacting PtR with k_{app} of $8.4 \times 10^{-4} \pm 0.6 \times 10^{-4}$ s^{-1} ($k_{app}[S94^{slow}]$) (Table 2).

To evaluate this puromycin reactivity, we used *M8:Ex1*-(*V85ns*) RNA, a *nonstop* RNA that is truncated at Val-85 codon (Fig. 3*A*), as a control of post-translocation step ribosome. A ribosome will translate a *nonstop* RNA up to the last codon on the mRNA and will remain in the post-translocation state until it is released from the mRNA (26, 27). Puromycin has been shown to react most efficiently with PtR at the post-translocation state, in which PtR resides in the P-site whereas the A-site is vacant (20, 21). Puromycin reaction of PtR(V85*ns*), which is produced with *M8:Ex1*(*V85ns*) RNA, was generally fast both in the presence and absence of AdoMet (Fig. 3*D*, *F*). In this case, the time course of puromycin reaction followed a three-component model (Equation 3, "Experimental Procedures"), rather than a two-component model (22). Fitting to the three-component model showed that ~70% of PtR exhibited k_{app} of 0.59 ± 0.10 s^{-1} in the absence of AdoMet ($k_{app}[V85ns^{-AdoMet}]$) (Table 2). We consider this value to be puromycin reactivity of the post-translocation state ribosome and will refer to it as $k_{app}(Post)$. This value was not significantly different from the corresponding $k_{app}(V85ns^{+AdoMet})$ obtained in the presence of AdoMet (Table 2). The remaining 30% of PtR showed much lower puromycin reactivity. Although we do not know in what state these PtR exist, accumulation of similar slow-reacting PtR on *nonstop* RNA was also reported in another system (27).

Approximately 10% of PtR(S94) were in the fast-reacting state. Although the observed S.E. was large, and statistical analysis would not be valid, the $k_{app}(S94^{fast})$ was similar to

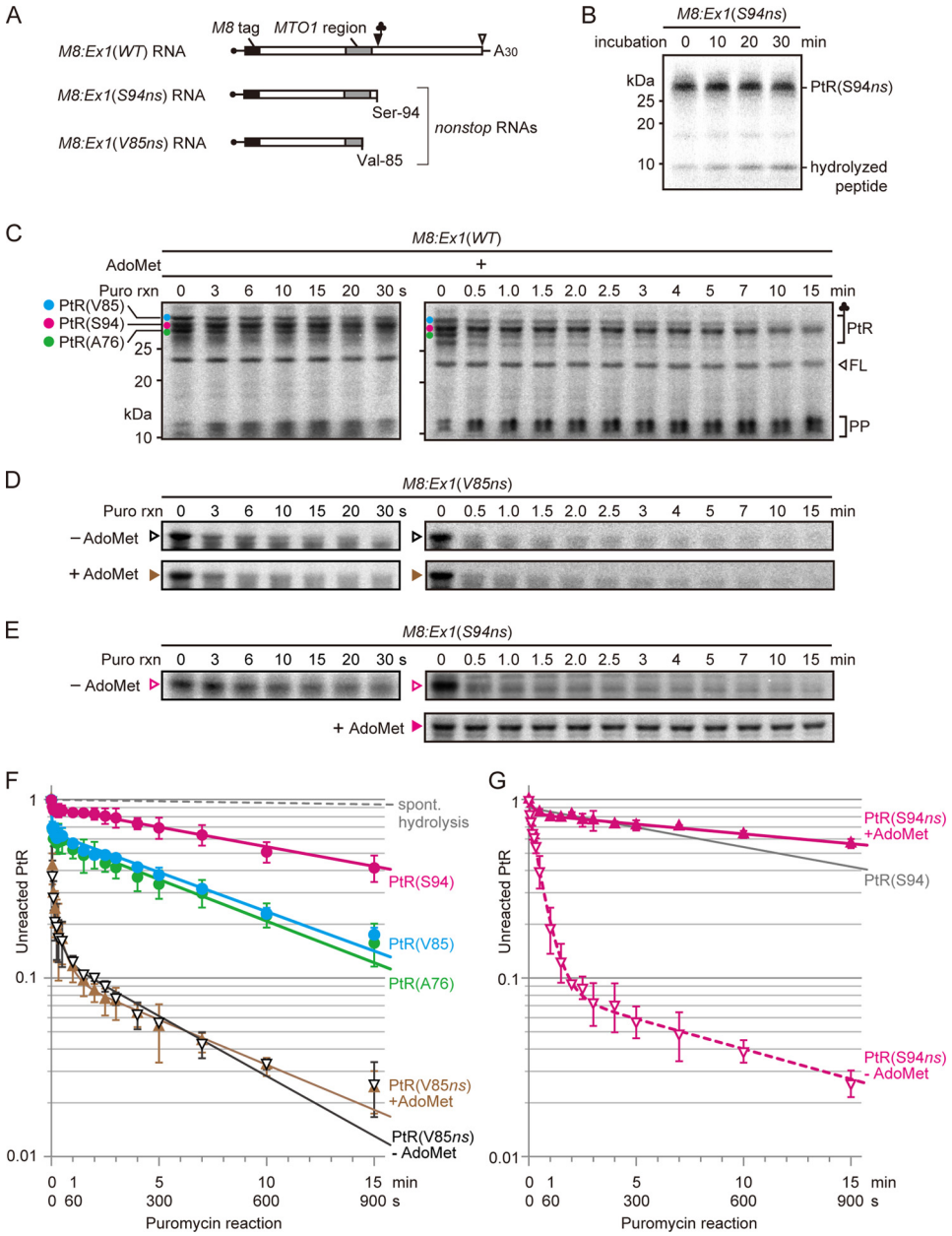

FIGURE 3. **Puromycin reactivities of stalled ribosomes.** *A*, schematic representation of *M8:Ex1*(*WT*) RNA and the 3′-truncated *nonstop* RNAs *M8:Ex1*(*S94ns*) and *M8:Ex1*(*V85ns*). *B*, stability of PtR(S94*ns*) in the translation reaction conditions used in the present study was analyzed. *M8:Ex1*(*S94ns*) RNA (100 fmol μl^{-1}) was translated in the absence of AdoMet. Translation reaction started at −10 min, and edeine, an inhibitor of translation initiation, was added at a final concentration of 2.5 mM at −5 min. Samples were removed at the indicated times for SDS-PAGE. Positions of PtR(S94*ns*) and the hydrolyzed peptide are marked. *C*, *M8:Ex1*(*WT*) RNA (50 fmol μl^{-1}) was translated in the presence of 1 mM AdoMet. After 30 min of translation, puromycin was added to a final concentration of 2 mM. At the indicated times, samples were removed for SDS-PAGE. The AdoMet-dependent PtR(S94) (*magenta circle*), PtR(V85) (*blue circle*) and PtR(A76) (*green circle*), the 21-kDa full-length translation product (*FL*), and peptidyl-puromycin (*PP*) bands are marked. *D* and *E*, *M8:Ex1*(*V85ns*) RNA (*D*) or *M8:Ex1*(*S94ns*) RNA (*E*) (100 fmol μl^{-1}) was translated in the presence or absence of 1 mM AdoMet and subjected to SDS-PAGE as in *C*. A representative result of triplicated experiments is shown in *B–E*. Positions of PtR(V85*ns*) and PtR(S94*ns*) are marked in *D* and *E*, respectively. *F*, radioactive signals in *B–D* were quantified. For each time point, the intensity of unreacted PtR was normalized to that at time 0. Average ± S.D. ($n = 3$) are shown. *Filled circles*, fraction of unreacted PtRs in *C*; *filled* and *open triangles*, fraction of unreacted PtR(V85*ns*) in the presence and absence of AdoMet, respectively, in *D*; *gray dashed line*, spontaneous hydrolysis in *B*. *G*, radioactive signals of unreacted PtR in *E* were quantified and presented as in *F*. *Filled* and *open triangles*, fraction of unreacted PtR(S94*ns*) in the presence and absence of AdoMet, respectively, in *E*. Puromycin reaction of PtR(S94) in *F* is reproduced for comparison (*gray line*).

k_{app}(*Post*) (Table 2), suggesting that this 10% fraction was stalled at the post-translocation state.

Puromycin Reactivity of the Stacked Second and Third Ribosomes—Puromycin reactivities of PtR(V85) and PtR(A76) followed a similar time course (Fig. 3, *C* and *F*). In the case of PtR(V85), fitting to the two-component model showed 36% fast-reacting and 64% slow-reacting PtR with k_{app} of 0.54 ± 0.11 s^{-1} ($k_{app}[V85^{fast}]$) and 1.7 × 10^{-3} ± 0.1 × 10^{-4} s^{-1} ($k_{app}[V85^{slow}]$) (Table 2), respectively. Similar values were obtained with PtR(A76) (Table 2). The $k_{app}(V85^{fast})$ and $k_{app}(A76^{fast})$ were not significantly different from k_{app}(*Post*) (Table 2), whereas $k_{app}(V85^{slow})$ and $k_{app}(A76^{slow})$ were significantly larger than $k_{app}(S94^{slow})$ ($p < 0.05$, Welch's *t* test).

TABLE 2
k_{app} values and the fractions of ribosomes showing the indicated puromycin reactivity

PtR	AdoMet	Fraction ± S.E.	k_{app} ± S.E.	Note[a]	*t* test for k_{app}[b]	
					$k_{app}(S94ns^{+AdoMet})$	$k_{app}(V85ns^{-AdoMet})$
		%	s^{-1}			
***M8:Ex1*(*WT*) RNA**						
PtR(S94)	+	10.3 ± 1.3	0.6 ± 0.7	$k_{app}(S94^{fast})$	−	−
		89.7 ± 1.3	$8.4 \times 10^{-4} \pm 0.6 \times 10^{-4}$	$k_{app}(S94^{slow})$	*	*
PtR(V85)	+	35.8 ± 1.0	0.54 ± 0.11	$k_{app}(V85^{fast})$	*	
		64.2 ± 1.0	$1.7 \times 10^{-3} \pm 0.1 \times 10^{-4}$	$k_{app}(V85^{slow})$	*	*
PtR(A76)	+	39.3 ± 1.6	0.54 ± 0.16	$k_{app}(A76^{fast})$	*	
		60.7 ± 1.6	$1.8 \times 10^{-3} \pm 0.2 \times 10^{-3}$	$k_{app}(A76^{slow})$	*	*
***M8:Ex1*(*V85ns*) RNA**						
PtR(V85*ns*)	+	70.4 ± 5.1	0.51 ± 0.09	$k_{app}(V85ns^{+AdoMet})$	*	
		19.3 ± 4.8	$3.8 \times 10^{-2} \pm 1.9 \times 10^{-2}$			*
		10.3 ± 7.0	$1.9 \times 10^{-3} \pm 1.1 \times 10^{-3}$			*
PtR(V85*ns*)	−	71.0 ± 5.0	0.59 ± 0.10	$k_{app}(V85ns^{-AdoMet})$	*	$k_{app}(Post)$
		15.6 ± 4.7	$5.2 \times 10^{-2} \pm 2.7 \times 10^{-2}$			*
		13.4 ± 6.9	$2.6 \times 10^{-3} \pm 0.8 \times 10^{-3}$		*	*
***M8:Ex1*(*S94ns*) RNA**						
PtR(S94*ns*)	+	17.6 ± 1.4	$6.0 \times 10^{-2} \pm 3.1 \times 10^{-2}$			*
		82.4 ± 1.4	$4.2 \times 10^{-4} \pm 0.5 \times 10^{-4}$	$k_{app}(S94ns^{+AdoMet})$	$k_{app}(Pre)$	*
PtR(S94*ns*)	−	10.2 ± 3.3	0.9 ± 1.5		−	−
		81.0 ± 3.4	$3.1 \times 10^{-2} \pm 0.3 \times 10^{-2}$	$k_{app}(S94ns^{-AdoMet})$	*	*
		8.7 ± 4.7	$1.3 \times 10^{-3} \pm 0.9 \times 10^{-3}$			*

[a] Those k_{app} values that constitute the major fraction and that are discussed in the text are named as indicated.
[b] Asterisks indicate significant difference ($p < 0.05$, Welch's *t* test with multiple test correction). − denotes that the S.E. was large, and the data were excluded from statistical analysis; their k_{app} values are shown here for reference.

Puromycin Reactivity of the PtR(S94ns) Formed on M8:Ex1(S94ns) RNA—When *M8:Ex1*(*S94ns*), a *nonstop* RNA that is truncated at the Ser-94 codon (Fig. 3*A*), was translated in the presence of AdoMet (Fig. 3*E, G*), puromycin reaction followed a time course similar to that of AdoMet-arrested PtR(S94), with >80% of PtR showing k_{app} of $4.2 \times 10^{-4} \pm 0.5 \times 10^{-4}$ s^{-1} ($k_{app}[S94ns^{+AdoMet}]$), suggesting that the ribosomes that translated Ser-94 *nonstop* RNA in the presence of AdoMet were in a state similar to that of the AdoMet-arrested ribosome. In contrast, when the same RNA was translated in the absence of AdoMet, the overall puromycin reaction was much faster than that in its presence (Fig. 3*E, G*). Fitting to the three-component model showed that >80% of the PtR exhibited k_{app} of $3.1 \times 10^{-2} \pm 0.3 \times 10^{-2}$ s^{-1} ($k_{app}[S94ns^{-AdoMet}]$), which is intermediate between $k_{app}(S94^{slow})$ *and* $k_{app}(Post)$ (Table 2).

The mto1–1 Mutation Speeds the Puromycin Reaction in the Presence of AdoMet—The MTO1 region acts in *cis* in AdoMet-induced translation arrest, and the *mto1–1* mutation, a Gly-84 to Ser substitution within the MTO1 region, abolishes the arrest (11). When *M8:Ex1*(*mto1–1*) RNA (Fig. 4*A*) was translated in the presence of AdoMet, none of the PtRs were detected, and the full-length translation product was found irrespective of the presence or absence of AdoMet (Fig. 4*B*, *lanes 3* and *4*), confirming that *mto1–1* mutation abolishes AdoMet-induced translation arrest (9, 11).

To test whether the low puromycin reactivity of PtR(S94*ns*) produced by translation of *M8:Ex1*(*S94ns*) RNA in the presence of AdoMet was dependent on MTO1 function, *M8:Ex1*-(*mto1–1*, *S94ns*) RNA was translated in the presence and absence of AdoMet, and puromycin reactivity was analyzed (Fig. 4, *C* and *D*). The results showed that puromycin reactivity of PtR(S94*ns*) formed on *M8:Ex1*(*mto1–1*, *S94ns*) RNA was not appreciably different between the presence and absence of AdoMet ($p > 0.05$, Welch's *t* test). These findings indicated that the slow puromycin reactivity of *M8:Ex1*(*S94ns*) RNA in the presence of AdoMet was dependent on MTO1 function.

To test if synthetic MTO1 peptide affects puromycin reactivity of PtRs, puromycin reaction was carried out in the presence of synthetic peptide of the MTO1 region. As a control, we also used a synthetic peptide harboring the *mto1–1* mutation (Fig. 5*A*). The results showed that the MTO1 region peptide did not affect the puromycin reactivity of any of the PtRs on *M8:Ex1*(*WT*) RNA (Fig. 5*B*, *C*). The result is consistent with our previous report that the MTO1 region acts inside the ribosomal exit tunnel (17).

Ribosome Stacking and Induction of CGS1 mRNA Degradation—We previously reported that AdoMet-induced translation arrest caused mRNA degradation events at multiple sites; a ladder of 5′-truncated species of *CGS1* mRNA formed as degradation intermediates, and their 5′-ends were separated by roughly 30 nt from each other (12). Finer evaluation of these RNA species using *M8:Ex1*(*WT*) RNA in this study (Fig. 6) showed that the 5′-ends of the smallest mRNA degradation intermediate (DI-1) was located 13–14 nt upstream of the A-site of the AdoMet-arrested ribosome. The second (DI-2) and third (DI-3) smallest ones exhibited twin peaks at 42/45 nt and at 69/72 nt, respectively, upstream of the A-site of the AdoMet-arrested ribosome. The distances between DI-1 and the upper and lower ends of the DI-2 twin peaks were 31–32 and 28–29 nt, respectively, whereas the DI-2 and DI-3 twin peaks were separated by 27 nt. Notably, the twin peaks of DI-2 were most prominently observed.

DISCUSSION

Tight Packing in an Array of Stacked Ribosomes on CGS1 mRNA—We detected multiple PtR species when *M8:Ex1*(*WT*) RNA was translated in the presence of AdoMet. We previously reported that AdoMet-induced translation arrest occurs at Ser-94 (11), and in the present study we determined that stacked second and third ribosomes harbored PtR(V85) and PtR(A76), respectively.

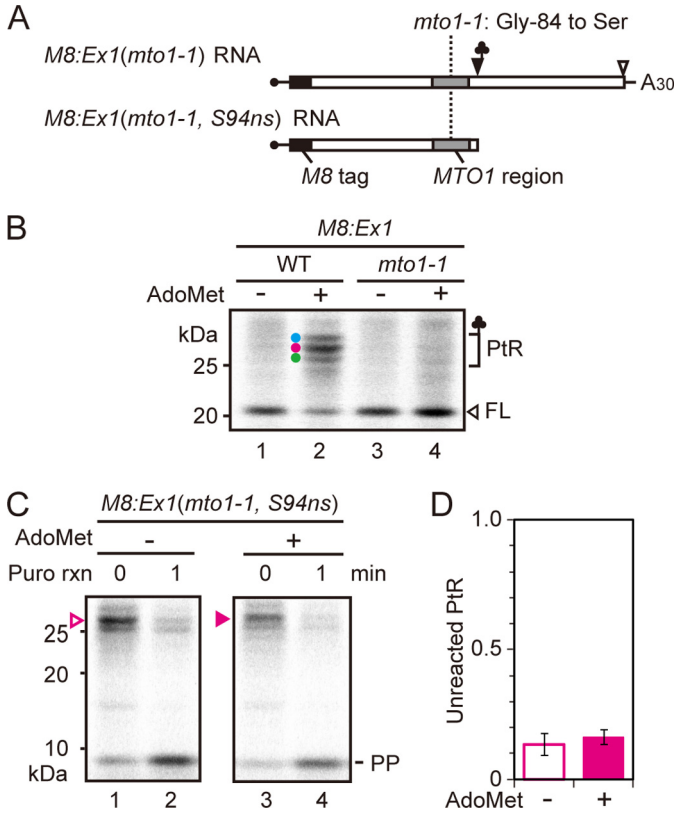

FIGURE 4. **Effect of *mto1–1* mutation on puromycin reaction.** *A*, schematic representation of *M8:Ex1*(*mto1–1*) and *M8:Ex1*(*mto1–1, S94ns*) RNA. *B*, *M8:Ex1*(*WT*) or *M8:Ex1*(*mto1–1*) RNA (50 fmol μl^{-1}) was translated in the absence (*lanes 1* and *3*) or presence (*lanes 2* and *4*) of 1 mM AdoMet. After 30 min of translation, samples were subjected to SDS-PAGE. The AdoMet-dependent PtRs and the full-length translation product (*FL*) are marked. *C*, *M8:Ex1*(*mto1–1, S94ns*) RNA (100 fmol μl^{-1}) was translated in the absence (*lanes 1* and *2*) or presence (*lanes 3* and *4*) of 1 mM AdoMet. After 30 min of translation, puromycin was added to a final concentration of 2 mM. Samples were removed for SDS-PAGE before (0 min) and 1 min after the start of puromycin reaction. The positions of PtR(S94*ns*) and peptidyl-puromycin (*PP*) bands are marked. A representative result of triplicated experiments is shown. *D*, radioactive signals in *C* were quantified. The intensity of unreacted PtR was normalized to that at time 0. Average ± S.D. ($n = 3$) are shown.

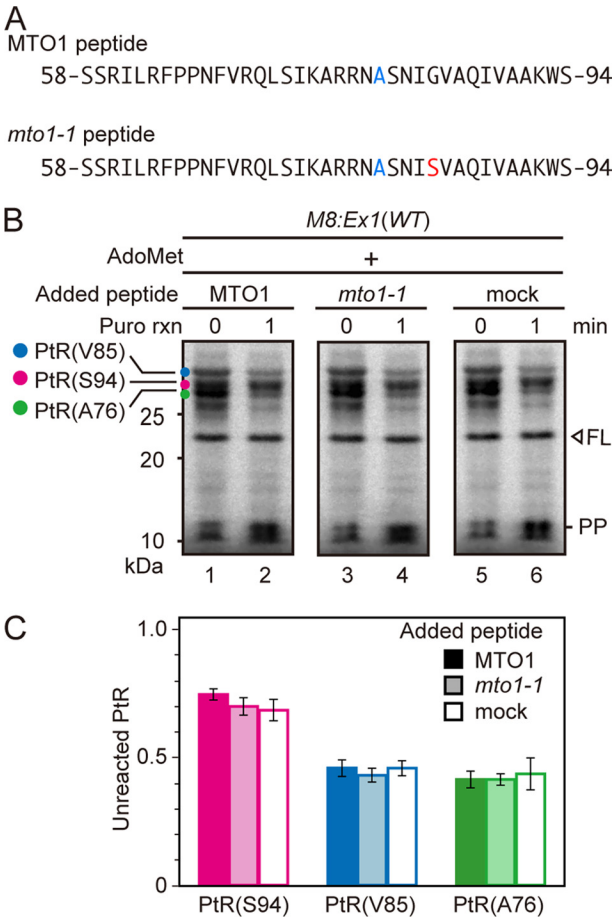

FIGURE 5. **Effect of exogenously added peptide covering the MTO1 region on puromycin reaction.** *A*, amino acid sequences of the synthetic peptides carrying wild-type MTO1 region (*upper panel*) and that with *mto1–1* mutation (*lower panel*). The *mto1–1* mutation is marked in *red*. To prevent dimerization, a Cys-80 to alanine substitution was introduced (marked in *blue*), which is among the few substitutions that are tolerated within the MTO1 region (25). *B*, *M8:Ex1*(*WT*) RNA (50 fmol μl^{-1}) was translated in the presence of 1 mM AdoMet with 500 nM synthetic peptide carrying wild-type MTO1 sequence or *mto1–1* mutation, or without synthetic peptide (mock). After 30 min of translation, puromycin was added to a final concentration of 2 mM. Samples were removed for SDS-PAGE before (0 min) and 1 min after the start of puromycin reaction. The AdoMet-dependent PtRs, the full-length translation product (*FL*) and peptidyl-puromycin (*PP*) bands are marked. A representative result of triplicated experiments is shown. *C*, radioactive signals in *B* were quantified. The intensity of unreacted PtR was normalized to that at time 0. Average ± S.D. ($n = 3$) are shown.

X-ray crystallographic studies of prokaryotic ribosomes showed that the mRNA cavity on the small subunit covered ~30 nt of mRNA (28, 29), corroborating the report that the length of mRNA protected from RNase digestion by a eukaryotic translating ribosome was about 30 nt (3, 6). The only available experimental data on stacked ribosomes came from RNase protection experiments which showed a ladder of protected RNA fragments, with the mRNA protected by a ribosome calculated to be 27–29 nt in WGE (8). However, no experimental study had reported on the exact intervals of the stacked ribosomes in terms of codons.

The anticodon end of a PtR can be positioned either in the A-site or P-site of the small subunit. We determined that the stacked second ribosome bore PtR(V85), but in which site, A or P, was it located? Because majority (90%) of PtR(S94) is located in the A-site of the small subunit of the arrested ribosome (11), if PtR(V85) on the stacked second ribosome is also located in the small subunit A-site, the A-site-to-A-site distance would be nine codons (Fig. 7*A*), whereas if PtR(V85) is located in the small subunit P-site, the A-site-to-A-site distance would be eight codons. Available data from the literature are limited to evaluate these two possibilities; however, an A-site-to-A-site distance of eight codons seems too small for the length of mRNA that is "held" by a ribosome (3, 6, 8). Thus, the most likely interpretation of our data is that PtR(V85) on the stacked second ribosome was located in the small subunit A-site, giving an A-site-to-A-site distance of nine codons between the arrested and stacked second ribosomes (Fig. 7*A*). Given that the PtR(V85) on the stacked second ribosome is located in the small subunit A-site, the same logic applies to the distance between the stacked second and third ribosomes, and the third ribosome would bear its PtR(A76) in the A-site of the small subunit (Fig. 7*A*).

Puromycin Reactivity of the AdoMet-arrested Ribosome—Puromycin reactivity has been used to monitor the PTC function in a number of ribosome arrest systems (27, 30–36). In all these systems, in which toeprint analysis was applied, PtR was

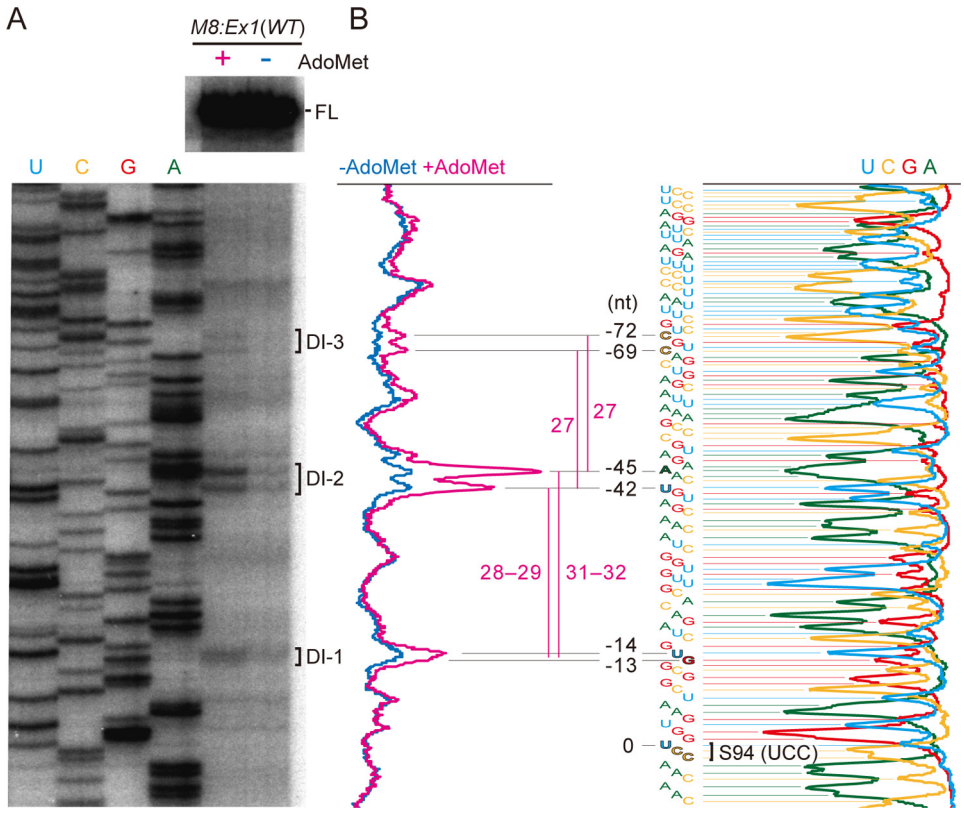

FIGURE 6. **Detection of the 5′-ends of degradation intermediates.** *A*, *M8:Ex1*(*WT*) RNA was translated in the presence (+) or absence (−) of AdoMet for 120 min. RNA was extracted and subjected to primer extension experiments. The samples were run on a sequencing gel along with a sequence ladder (the lanes are labeled as mRNA sequence). The peaks of the 5′-end positions are marked as DI-1, DI-2, and DI-3 in order of increasing size. A representative result of duplicated experiments is shown. *B*, scanned data of *A* are presented. The numbers indicate the distances in nt from the A-site of the AdoMet-arrested ribosome (Ser-94 codon).

shown to be located in the P-site. In these systems, puromycin reaction was slow, which was interpreted as PTC activity was inhibited and/or puromycin could not readily access the PTC A-site. In the case of arginine attenuator peptide of *Neurospora crassa* (15, 24), PTC function was suggested to be interfered by the nascent peptide in the P-site and the presence of arginine (27). So, how can we explain the slow puromycin reaction in the *CGS1* system? PTC catalyzes the puromycin reaction when PtR resides in the P-site and puromycin comes into the A-site, whereas the AdoMet-arrested ribosome is stalled at the pre-translocation step and PtR resides in the A-site. Although no reports have examined puromycin reactivity of the A-site-bound PtR in eukaryotes, studies in prokaryotes have shown that puromycin reacts 1,000–3,000 times slower with pre-translocation step ribosomes than with post-translocation step ones (21), which would explain the low puromycin reactivity of AdoMet-arrested ribosomes in *CGS1*.

When *M8:Ex1*(*S94ns*) RNA was translated in the presence of AdoMet, $k_{app}(S94ns^{+AdoMet})$ was small and similar to $k_{app}(S94^{slow})$ (Table 2). This low reactivity is not a general effect of AdoMet application, because in the case of PtR(V85*ns*), puromycin reaction was fast irrespective of the AdoMet conditions. The result suggested that the ribosome that had translated the *M8:Ex1*(*S94ns*) RNA in the presence of AdoMet was in a state similar to the AdoMet-arrested ribosomes, not simply stopped at the *nonstop* RNA end. This interpretation is consistent with our previously reported PEGylation assay showing nascent CGS1 peptide compaction in the ribosomes that have translated Ser-94 *nonstop* RNA (17). Notably, however, $k_{app}(S94ns^{+AdoMet})$ was significantly smaller than $k_{app}(S94^{slow})$ (Table 2). PtR(S94) formed on *M8:Ex1*(*WT*) RNA can resume translation during the 15-min puromycin reaction period, and the ribosome will pass through the post-translocation state, during which puromycin reaction is efficient, whereas resumption of translation could be blocked on the *nonstop* RNA. If this assumption is granted, the $k_{app}(S94ns^{+AdoMet})$ of $4.2 \times 10^{-4} \pm 0.5 \times 10^{-4}$ s^{-1} represents the puromycin reactivity of pre-translocation state ribosomes, which we will refer to $k_{app}(Pre)$. Corroborating the report in the purified *E. coli in vitro* translation system mentioned above (21), $k_{app}(Pre)$ is ~1,400 times smaller than $k_{app}(Post)$.

When *M8:Ex1*(*S94ns*) RNA was translated in the absence of AdoMet, $k_{app}(S94ns^{-AdoMet})$ was intermediate between $k_{app}(Pre)$ and $k_{app}(Post)$. In *E. coli*, puromycin reactivity of the A/P hybrid state ribosomes was ~10-fold lower than that of the post-translocation state ones (21, 37, 38). This coincidence suggests that $k_{app}(S94ns^{-AdoMet})$ of $3.1 \times 10^{-2} \pm 0.3 \times 10^{-2}$ s^{-1} represents the puromycin reactivity of the A/P hybrid state ribosomes.

Puromycin Reactivity of PtR on the Stacked Second and Third Ribosomes—Puromycin reactivity of the stacked second and third ribosomes showed that the ribosomes are composed of two fractions: (i) The majority (~60%) of the ribosomes exhibited $k_{app}(V85^{slow})$ and (ii) ~40% exhibited $k_{app}(V85^{fast})$. Let us

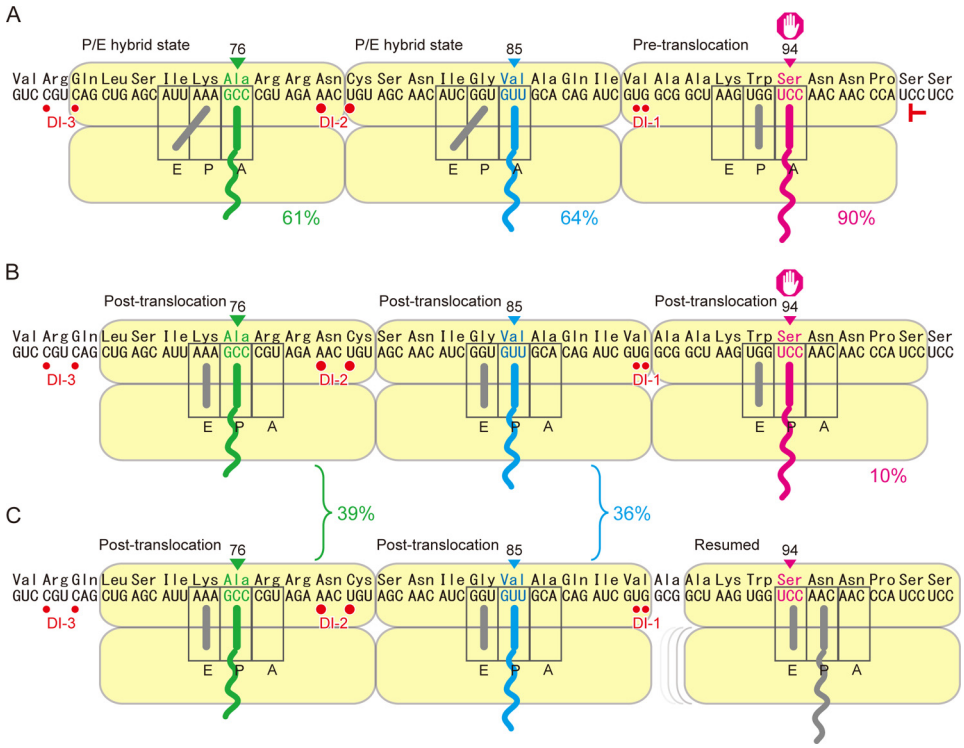

FIGURE 7. **Models for the positions and states of the ribosomes in a stacked array.** *Red T* marks the position of the toeprint signal (11). *Red circles* mark the 5′-ends of the degradation intermediates, DI-1, DI-2, and DI-3 (Fig. 6). Each ribosome is drawn to cover nine codons of mRNA. *A*, the stacked second and third ribosomes are in the P/E hybrid state, with the anticodon ends of their PtRs located in the A-site, whereas the AdoMet-arrested one is in the pre-translocation step. *B*, the AdoMet-arrested and stacked second and third ribosomes are all in the post-translocation state. *C*, the AdoMet-arrested ribosome has resumed translation, whereas the stacked ribosomes are still there after one round of translocation. The approximate percentages of the ribosomes in each state are presented.

consider the majority first. The $k_{app}(V85^{slow})$ was similar to but significantly larger than $k_{app}(Pre)$ (Table 2). During translocation, a ribosome undergoes several conformation changes, which include rotation of the small subunit relative to the large subunit (39, 40), rotation of the head of the small subunit (40, 41), and conformation changes of the ribosomal protein L1 stalk to facilitate tRNA release from the E-site (40, 42). Notably, upon transition to the hybrid state, rotation of the small subunit occurs (41). When a ribosome collides with the preceding one, some of these conformation changes might be hindered, and the ribosome may stall during translocation either in the P/E or A/P hybrid state. As discussed above, $k_{app}(S94ns^{-AdoMet})$ likely represents the puromycin reactivity of A/P hybrid state, which is significantly larger than $k_{app}(V85^{slow})$ ($p < 0.05$, Welch's t test). we can reasonably expect that puromycin reactivity of the P/E hybrid state is as low as that of pre-translocation step, because the peptidyl-tRNA occupies the A-site as in the pre-translocation step. In *E. coli*, experiments using viomycin, which inhibits translocation at the P/E hybrid state, showed that puromycin reactivity of the P/E hybrid state was ~2-fold higher than in the pre-translocation state (21). Therefore, we may infer that the majority of the stacked second and third ribosomes are in the P/E hybrid state (Fig. 7*A*).

Next, consider the ~40% of the stacked ribosomes. The $k_{app}(V85^{fast})$ was not significantly different from $k_{app}(Post)$ (Table 2), suggesting that these ribosomes are in the post-translocation state. As discussed in the previous section, occupation of PtR(V85) in the small subunit P-site would be too short of a distance between the arrested and stacked ribosomes. Because 10% of the PtR(S94) are likely in the post-translocation state, a corresponding fraction of PtR(V85) is stacked behind the P-site-arrested ribosome, resulting in a nine-codon interval (Fig. 7*B*). Then, we must address the remainder of the PtR(V85). For the stacked ribosomes to stall at the post-translocation state and are prevented from proceeding to the peptidyltransfer step, either the release of eEF-2 or the incorporation of aminoacyl-tRNA must be inhibited (21, 43). In prokaryotes, post-translocation state ribosomes with associated EF-G exhibit full puromycin reactivity, although entry of aminoacyl-tRNA is possible only after dissociation of EF-G (21, 38). This logic reveals an explanation for the remaining PtR(V85): the leading ribosome had initially arrested at Ser-94 and the second ribosome stacked at Val-85, but the leading ribosome has resumed translation (and thus was no longer detected at the Ser-94 position) before the start of puromycin reaction (Fig. 7*C*). In this scenario, the second ribosome sitting at Val-85 has gone one round of translocation to be in the post-translocation state. The prokaryotic L7/L12 (eukaryotic P0/P1) stalk, which is located near the factor binding site of the large subunit, is thought to function in accommodating translation factors including aminoacyl-tRNA (44, 45, 46). Ribosomal collision may hinder one of these functions.

Ribosome Stacking and CGS1 mRNA Degradation—In the present study, we carried out precise mapping of the 5′ ends of the degradation intermediates (Fig. 6). DI-2 and DI-3 are separated by 27 nt, or nine codons, corroborating the distance

between the PtR codons of the stacked second and third ribosomes (Fig. 7*A*). Our previous polysome profiling experiment showed that DI-1 is predominantly found in the monosome fraction, and DI-2 and DI-3 are found in two- and three-ribosome fractions, respectively (12). The nine-codon distance between DI-2 and DI-3 strongly suggests that the stacked second and third ribosomes are responsible for determining the positions of DI-2 and DI-3, respectively (Fig. 7*A*). Notably, DI-2 was detected most strongly, suggesting that ribosome collision has a role in inducing the mRNA degradation. Understanding mRNA cleavage defined by stacked ribosomes will shed light on the important regulatory roles that stacked ribosomes play in the control of mRNA degradation.

Acknowledgments—We thank Drs. Yukako Chiba, Yuka Hagiwara-Komoda, Haruhide Mori, and Derek Bartlem of Hokkaido University for valuable comments on this study. We also thank Saeko Yasokawa for skillful technical assistance and Kumi Fujiwara, Naoe Konno, and Maki Mori for general assistance. We used the Radioisotope Laboratory and DNA Sequencing Facility of the Graduate School of Agriculture, Hokkaido University.

REFERENCES

1. Martin, K. A., and Miller, O. L. Jr. (1983) Polysome structure in sea urchin eggs and embryos: an electron microscopic analysis. *Dev. Biol.* **98,** 338–348
2. Kopeina, G. S., Afonina, Z. A., Gromova, K. V., Shirokov, V. A., Vasiliev, V. D., and Spirin, A. S. (2008) Step-wise formation of eukaryotic double-row polyribosomes and circular translation of polysomal mRNA. *Nucleic Acids Res.* **36,** 2476–2488
3. Ingolia, N. T., Ghaemmaghami, S., Newman, J. R., and Weissman, J. S. (2009) Genome-wide analysis in vivo of translation with nucleotide resolution using ribosome profiling. *Science* **324,** 218–223
4. Brandt, F., Etchells, S. A., Ortiz, J. O., Elcock, A. H., Hartl, F. U., and Baumeister, W. (2009) The native 3D organization of bacterial polysomes. *Cell* **136,** 261–271
5. Brandt, F., Carlson, L. A., Hartl, F. U., Baumeister, W., and Grünewald, K. (2010) The three-dimensional organization of polyribosomes in intact human cells. *Mol. Cell* **39,** 560–569
6. Ingolia, N. T., Lareau, L. F., and Weissman, J. S. (2011) Ribosome profiling of mouse embryonic stem cells reveals the complexity and dynamics of mammalian proteomes. *Cell* **147,** 789–802
7. Afonina, Zh. A., Myasnikov, A. G., Khabibullina, N. F., Belorusova, A. Y., Menetret, J. F., Vasiliev, V. D., Klaholz, B. P., Shirokov, V. A., and Spirin, A. S. (2013) Topology of mRNA chain in isolated eukaryotic double-row polyribosomes. *Biochemistry* **78,** 445–454
8. Wolin, S. L., and Walter, P. (1988) Ribosome pausing and stacking during translation of a eukaryotic mRNA. *EMBO J.* **7,** 3559–3569
9. Chiba, Y., Ishikawa, M., Kijima, F., Tyson, R. H., Kim, J., Yamamoto, A., Nambara, E., Leustek, T., Wallsgrove, R. M., and Naito, S. (1999) Evidence for autoregulation of cystathionine γ-synthase mRNA stability in *Arabidopsis*. *Science* **286,** 1371–1374
10. Chiba, Y., Sakurai, R., Yoshino, M., Ominato, K., Ishikawa, M., Onouchi, H., and Naito, S. (2003) *S*-Adenosyl-L-methionine is an effector in the posttranscriptional autoregulation of the cystathionine γ-synthase gene in *Arabidopsis*. *Proc. Natl. Acad. Sci. U.S.A.* **100,** 10225–10230
11. Onouchi, H., Nagami, Y., Haraguchi, Y., Nakamoto, M., Nishimura, Y., Sakurai, R., Nagao, N., Kawasaki, D., Kadokura, Y., and Naito, S. (2005) Nascent peptide-mediated translation elongation arrest coupled with mRNA degradation in the *CGS1* gene of *Arabidopsis*. *Genes Dev.* **19,** 1799–1810
12. Haraguchi, Y., Kadokura, Y., Nakamoto, M., Onouchi, H., and Naito, S. (2008) Ribosome stacking defines *CGS1* mRNA degradation sites during nascent peptide-mediated translation arrest. *Plant Cell Physiol.* **49,** 314–323
13. Budkevich, T., Giesebrecht, J., Altman, R. B., Munro, J. B., Mielke, T., Nierhaus, K. H., Blanchard, S. C., and Spahn, C. M. (2011) Structure and dynamics of the mammalian ribosomal pretranslocation complex. *Mol. Cell* **44,** 214–224
14. Tsuboi, T., Kuroha, K., Kudo, K., Makino, S., Inoue, E., Kashima, I., and Inada, T. (2012) Dom34:hbs1 plays a general role in quality-control systems by dissociation of a stalled ribosome at the 3′ end of aberrant mRNA. *Mol. Cell* **46,** 518–529
15. Wang, Z., and Sachs, M. S. (1997) Ribosome stalling is responsible for arginine-specific translational attenuation in *Neurospora crassa*. *Mol. Cell Biol.* **17,** 4904–4913
16. Sachs, M. S., Wang, Z., Gaba, A., Fang, P., Belk, J., Ganesan, R., Amrani, N., and Jacobson, A. (2002) Toeprint analysis of the positioning of translation apparatus components at initiation and termination codons of fungal mRNAs. *Methods* **26,** 105–114
17. Onoue, N., Yamashita, Y., Nagao, N., Goto, D. B., Onouchi, H., and Naito, S. (2011) *S*-Adenosyl-L-methionine induces compaction of nascent peptide chain inside the ribosomal exit tunnel upon translation arrest in the *Arabidopsis CGS1* gene. *J. Biol. Chem.* **286,** 14903–14912
18. Ho, S. N., Hunt, H. D., Horton, R. M., Pullen, J. K., and Pease, L. R. (1989) Site-directed mutagenesis by overlap extension using the polymerase chain reaction. *Gene* **77,** 51–59
19. Pogulis, R. J., Vallejo, A. N., and Pease, L. R. (1996) In vitro recombination and mutagenesis by overlap extension PCR. *Methods Mol. Biol.* **57,** 167–176
20. Semenkov, Yu., Shapkina, T., Makhno, V., and Kirillov, S. (1992) Puromycin reaction for the A site-bound peptidyl-tRNA. *FEBS Lett.* **296,** 207–210
21. Pan, D., Kirillov, S. V., and Cooperman, B. S. (2007) Kinetically competent intermediates in the translocation step of protein synthesis. *Mol. Cell* **25,** 519–529
22. Akaike, H. (1974) A new look at the statistical model identification. *IEEE Trans. Automat. Contr.* **19,** 716–723
23. Benjamini, Y., and Hochberg, Y. (1995) Controlling the false discovery rate: a practical and powerful approach to multiple testing. *J. R. Stat. Soc. B.* **57,** 289–300
24. Fang, P., Wu, C., and Sachs, M. S. (2002) *Neurospora crassa* supersuppressor mutants are amber codon-specific. *Fungal Genet. Biol.* **36,** 167–175
25. Ominato, K., Akita, H., Suzuki, A., Kijima, F., Yoshino, T., Yoshino, M., Chiba, Y., Onouchi, H., and Naito, S. (2002) Identification of a short highly conserved amino acid sequence as the functional region required for post-transcriptional autoregulation of the cystathionine γ-synthase gene in *Arabidopsis*. *J. Biol. Chem.* **277,** 36380–36386
26. Ramu, H., Vázquez-Laslop, N., Klepacki, D., Dai, Q., Piccirilli, J., Micura, R., and Mankin, A. S. (2011) Nascent peptide in the ribosome exit tunnel affects functional properties of the A-site of the peptidyl transferase center. *Mol. Cell* **41,** 321–330
27. Wei, J., Wu, C., and Sachs, M. S. (2012) The arginine attenuator peptide interferes with the ribosome peptidyl transferase center. *Mol. Cell Biol.* **32,** 2396–2406
28. Yusupova, G. Z., Yusupov, M. M., Cate, J. H., and Noller, H. F. (2001) The path of messenger RNA through the ribosome. *Cell* **106,** 233–241
29. Jenner, L. B., Demeshkina, N., Yusupova, G., and Yusupov, M. (2010) Structural aspects of messenger RNA reading frame maintenance by the ribosome. *Nat. Struct. Mol. Biol.* **17,** 555–560
30. Cruz-Vera, L. R., Gong, M., and Yanofsky, C. (2006) Changes produced by bound tryptophan in the ribosome peptidyl transferase center in response to TnaC, a nascent leader peptide. *Proc. Natl. Acad. Sci. U.S.A.* **103,** 3598–3603
31. Muto, H., Nakatogawa, H., and Ito, K. (2006) Genetically encoded but nonpolypeptide prolyl-tRNA functions in the A site for SecM-mediated ribosomal stall. *Mol. Cell* **22,** 545–552
32. Vazquez-Laslop, N., Thum, C., and Mankin, A. S. (2008) Molecular mechanism of drug-dependent ribosome stalling. *Mol. Cell* **30,** 190–202
33. Chiba, S., and Ito, K. (2012) Multisite ribosomal stalling: a unique mode of regulatory nascent chain action revealed for MifM. *Mol. Cell* **47,** 863–872
34. Gong, F., Ito, K., Nakamura, Y., and Yanofsky, C. (2001) The mechanism of

tryptophan induction of tryptophanase operon expression: tryptophan inhibits release factor-mediated cleavage of TnaC-peptidyl-tRNA^{Pro}. *Proc. Natl. Acad. Sci. U.S.A.* **98,** 8997–9001
35. Muto, H., and Ito, K. (2008) Peptidyl-prolyl-tRNA at the ribosomal P-site reacts poorly with puromycin. *Biochem. Biophys. Res. Commun.* **366,** 1043–1047
36. Ito, K., and Chiba, S. (2013) Arrest peptides: *cis*-acting modulators of translation. *Annu. Rev. Biochem.* **82,** 171–202
37. Sharma, D., Southworth, D. R., and Green, R. (2004) EF-G-independent reactivity of a pre-translocation-state ribosome complex with the aminoacyl tRNA substrate puromycin supports an intermediate (hybrid) state of tRNA binding. *RNA* **10,** 102–113
38. Blanchard, S. C., Cooperman, B. S., and Wilson, D. N. (2010) Probing translation with small-molecule inhibitors. *Chem. Biol.* **17,** 633–645
39. Frank, J., and Agrawal, R. K. (2000) A ratchet-like inter-subunit reorganization of the ribosome during translocation. *Nature* **406,** 318–322
40. Ben-Shem, A., Jenner, L., Yusupova, G., and Yusupov, M. (2010) Crystal structure of the eukaryotic ribosome. *Science* **330,** 1203–1209
41. Fischer, N., Konevega, A. L., Wintermeyer, W., Rodnina, M. V., and Stark, H. (2010) Ribosome dynamics and tRNA movement by time-resolved electron cryomicroscopy. *Nature* **466,** 329–333
42. Andersen, C. B., Becker, T., Blau, M., Anand, M., Halic, M., Balar, B., Mielke, T., Boesen, T., Pedersen, J. S., Spahn, C. M., Kinzy, T. G., Andersen, G. R., and Beckmann, R. (2006) Structure of eEF3 and the mechanism of transfer RNA release from the E-site. *Nature* **443,** 663–668
43. Frank, J. (2012) Intermediate states during mRNA-tRNA translocation. *Curr. Opin. Struct. Biol.* **22,** 778–785
44. Wilson, D. N., and Nierhaus, K. H. (2005) Ribosomal proteins in the spotlight. *Crit. Rev. Biochem. Mol. Biol.* **40,** 243–267
45. Uchiumi, T., Honma, S., Nomura, T., Dabbs, E. R., and Hachimori, A. (2002) Translation elongation by a hybrid ribosome in which proteins at the GTPase center of the *Escherichia coli* ribosome are replaced with rat counterparts. *J. Biol. Chem.* **277,** 3857–3862
46. Diaconu, M., Kothe, U., Schlünzen, F., Fischer, N., Harms, J. M., Tonevitsky, A. G., Stark, H., Rodnina, M. V., and Wahl, M. C. (2005) Structural basis for the function of the ribosomal L7/12 stalk in factor binding and GTPase activation. *Cell* **121,** 991–1004